CHEMISTRY OF MATERIALS

ARTICLE

pubs.acs.org/cm

InP@ZnSeS, Core@Composition Gradient Shell Quantum Dots with Enhanced Stability

Jaehoon Lim,[†] Wan Ki Bae,[‡] Donggu Lee,[#] Min Ki Nam,[§] Joohyun Jung,[§] Changhee Lee,[#] Kookheon Char,[*,†] and Seonghoon Lee[*,§]

[†]School of Chemical and Biological Engineering, The National Creative Research Initiative Center for Intelligent Hybrids, Seoul National University, 599 Gwanak-ro, Gwanak-gu, Seoul 151-744, Korea

[‡]Chemistry Division, Los Alamos National Laboratory, Los Alamos, New Mexico 87545, United States

[§]School of Chemistry, Seoul National University, 599 Gwanak-ro, Gwanak-gu, Seoul 151-747, Korea

[#]School of Electrical Engineering and Computer Science, Inter-University Semiconductor Research Center (ISRC), Seoul National University, Seoul, 151-744, Korea

Supporting Information

ABSTRACT: Utilizing the reactivity difference between TOPSe and TOPS, we synthesized InP@ZnSeS QDs with the composition gradient in a radial direction where ZnSe alleviated lattice strain and ZnS protected QDs from degradation so that we achieved QDs with high QE and photo/chemical stability. In terms of systematic investigation on the relationship between the shell nanostructure and QD stability, we demonstrated that QDs with thick gradient shells exhibited high QE and much enhanced stability against the shell degradation under UV irradiation, ligand exchange, or rigorous purification. This enhanced stability of InP@ZnSeS QDs is attributed to the improved uniformity of composition gradient shells, the efficient confinement of exciton wavefunctions, and the minimized surface oxidation and non-radiative decay via surface states generated by photo-oxidation or ligand exchange. Using InP@ZnSeS QDs with enhanced stability, we were able to demonstrate InP-based colloidal green-emitting QD-LEDs. Although the current status of InP@ZnSeS QDs is not fully optimized to realize practical optoelectronic devices, the approach taken in the present study (i.e., the composition gradient shell structure naturally made from reactivity difference in precursors) will give clues to facilitate the synthesis of InP QDs with advanced nanostructures.

KEYWORDS: InP quantum dots, composition gradient shell, stability

Great attention has been given to colloidal quantum dots (QDs), not only because of their unique and superb optical properties (such as broad absorption, narrow emission spectral bandwidth, and easy bandgap tunability), but also because of their wide application potentials as a new type of phosphors in light-emitting devices[1] and biomarkers.[2] However, most of the previous fundamental studies and potential applications have been focused on Group II−VI QDs, which could impose critical constraints for practicable applications, because of the toxic elements (i.e., Cd and Hg) that constitute QDs. To avoid the potential limitations, QDs with different elements, for example, Group III−V (i.e., InP[3] and InAs[4]) or Group IV (i.e., Si[5]) QDs have been investigated. Among the possible material choices, InP QDs, in particular, have gained significant attention, because of their wide emission spectrum tunability ranging from the visible region to the near-infrared (NIR) region.

Recently, considerable progress in the synthesis of InP QDs has been made; however, their optical properties as well as photo/chemical stability are much inferior to relatively well-developed Group II−VI QDs (i.e., CdSe). Their inferior properties originate from harsh reaction control, which is due to more covalent bonding character as well as the difficulty in the surface passivation: stronger bond formation as well as the lack of suitable buffer layer between the InP core and the ZnS shell. The obstacles in the reactivity control as well as problems with the surface passivation, have recently been overcome through delicate control of the precursor ratio,[3e−g] additives,[3e] or temperature control;[3f] consequently, considerable quantum efficiency (QE, up to 70%) and color purity (fwhm below 45 nm) have resulted.[3f] Nevertheless, compressive lattice strain and reduced QE due to lattice-mismatched ZnS shell surface passivation must be resolved. Lattice strain with a ZnS shell limits a shell thickness to <1 nm. Such a thin shell is quite vulnerable against degradable conditions, leading to reduction in long-term photo/chemical stability. In order to improve stability of InP-based QDs, the shell thickness should be increased with a lattice adaptor, such as an alloyed or intermediate shell, in such a way to alleviate the lattice strain with a gradual change in shell lattice constant.[6] Among available materials, ZnSe

Received: June 1, 2011
Revised: August 12, 2011
Published: September 30, 2011

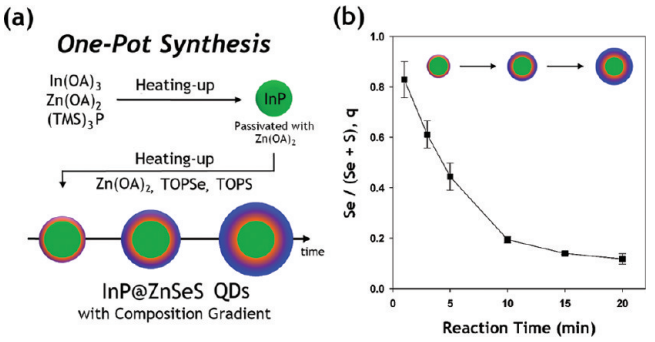

Figure 1. (a) Schematic of the synthetic procedure of InP@ZnSeS QDs. (b) Temporal evolution of the atomic ratio of Se (Se/(Se + S), q in ZnSeS shells during the shell growth with n = 2.

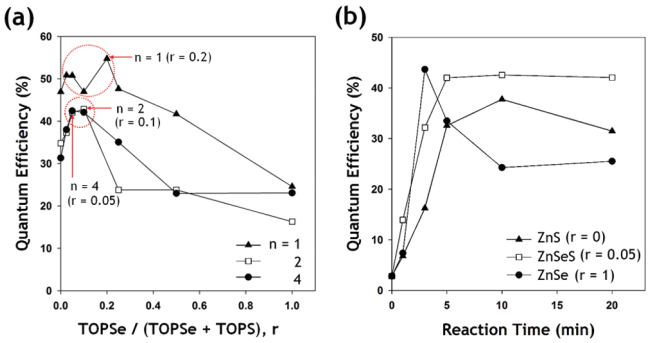

Figure 2. (a) PL QEs after the termination of reaction for InP@ZnSeS QDs, as a function of the amount of shell formation precursors (n) as well as the molar ratio of TOPSe (r) in the shell precursor solution. Dotted red circles represent the optimal range for a given n. Red arrows indicate each of the optimal points for r for a given n. (b) Temporal evolution of PL QE for (▲) InP@ZnS, (●) InP@ZnSe, and (□) InP@ZnSeS QDs, with n = 2.

is regarded as a proper choice for InP-based QDs, thanks to the low toxicity as well as a suitable lattice parameter.

To integrate ZnSe (alleviating lattice strain) and ZnS (protecting from degradation) and achieve QDs with high QE and photo/chemical stability, we introduce thick and uniform ZnSeS shells onto InP cores (InP@ZnSeS) in the form of the composition gradient in a radial direction. Because of the faster reaction rate of TOPSe than TOPS,[6] the composition gradient shells, where ZnSe is preferentially formed close to the InP core and the composition of ZnSe in the shell gradually decreases in the radial direction, are easily achieved with the simple addition of Se and S precursors all together (see Figure 1a), since the reactivity difference in precursors plays a role and, thus, reproducibility is remarkable. The composition and thickness in the shell were readily controlled by the amount of shell precursors (In:P:Zn:(Se + S) = 0.1:0.1:n:n (mmol), where n = 1, 2, and 4) as well as the molar ratio of TOPSe, r (here, r is defined as TOPSe/(TOPSe + TOPS), where $0 \leq r \leq 1$) in the precursor solutions. Temperature control, heating up from 200 to 300 °C, facilitates the formation of composition gradient ZnSeS shells. Detailed synthetic procedure and optical characterization are provided in the Supporting Information.

The existence of ZnSe in the ZnSeS shell is easily confirmed from the emission spectra (larger red shift with InP@ZnSeS QDs, compared with InP@ZnS QDs), but the spatial

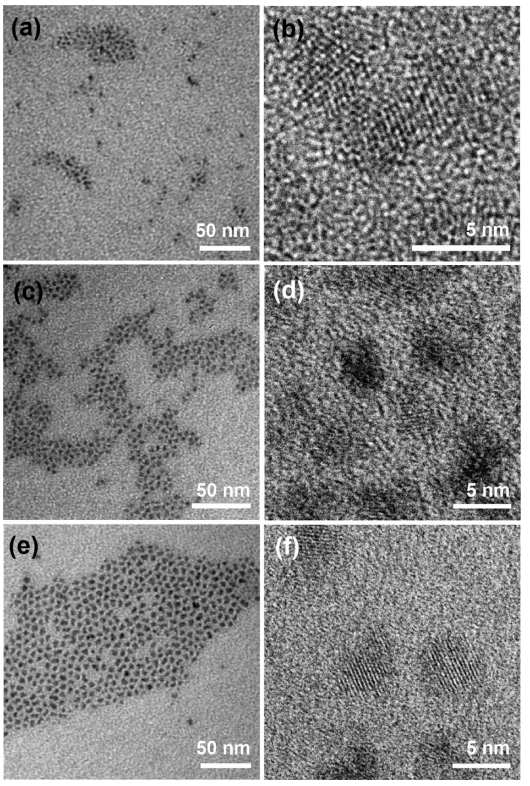

Figure 3. TEM images of InP@ZnSeS QDs with (a, b) n = 1, (c, d) n = 2, and (e, f) n = 4 with an optimal Se ratio (r).

distribution of ZnSe cannot be accurately determined. InP@ZnSeS and InP@ZnS QDs were made from the same pristine InP cores (see Figure S1 in the Supporting Information). To reveal the actual location and composition of Se, energy-dispersive X-ray analysis was conducted, as a function of reaction time (see Figure 1b and Table S1 in the Supporting Information). If ZnSe is assumed to be uniformly located in the ZnSeS shell, the atomic atomic ratio of Se in the shell, q, which is defined as Se/(Se + S) in the shell, should be constant during the entire reaction time. (Cf, r is defined as TOPSe/(TOPSe + TOPS) in the precursor solution). However, the gradual decrease in the Se atomic ratio (q) was observed, implying that Se is dominantly located near the InP core, whereas S increases in the radial direction of the shell. At the end of reaction, the Se atomic ratio (q) in the ZnSeS shell formed with r = 0.05 and n = 2 precursor solution was found to be 0.12, probably due to the lower reactivity of TOPS, compared with that of TOPSe. Since, in the present study, we did not observe any noticeable blue-shift of the UV−Vis or PL spectra during the reaction at 300 °C, the alloying of InP cores with shell components (i.e., Zn, Se or S) did not occur in the present reaction conditions, or was unnoticeable even if it occurred.

In conjunction with the relationship between lattice mismatch and shell growth behavior, the QDs formed with a high TOPSe molar ratio (r) should exhibit the highest QE at the end of reaction, because of the minimized lattice mismatch (for example, 3.4% for ZnSe and 7.7% for ZnS). However, we found that the optimal molar ratio of TOPSe (r) for the highest QEs were located in a narrow range (the dotted circle in Figure 2a) and that the QEs of InP@ZnSeS QDs at the optimal r values were approximately twice as high as those of InP@ZnSe QDs.

dx.doi.org/10.1021/cm201550w |Chem. Mater. 2011, 23, 4459–4463

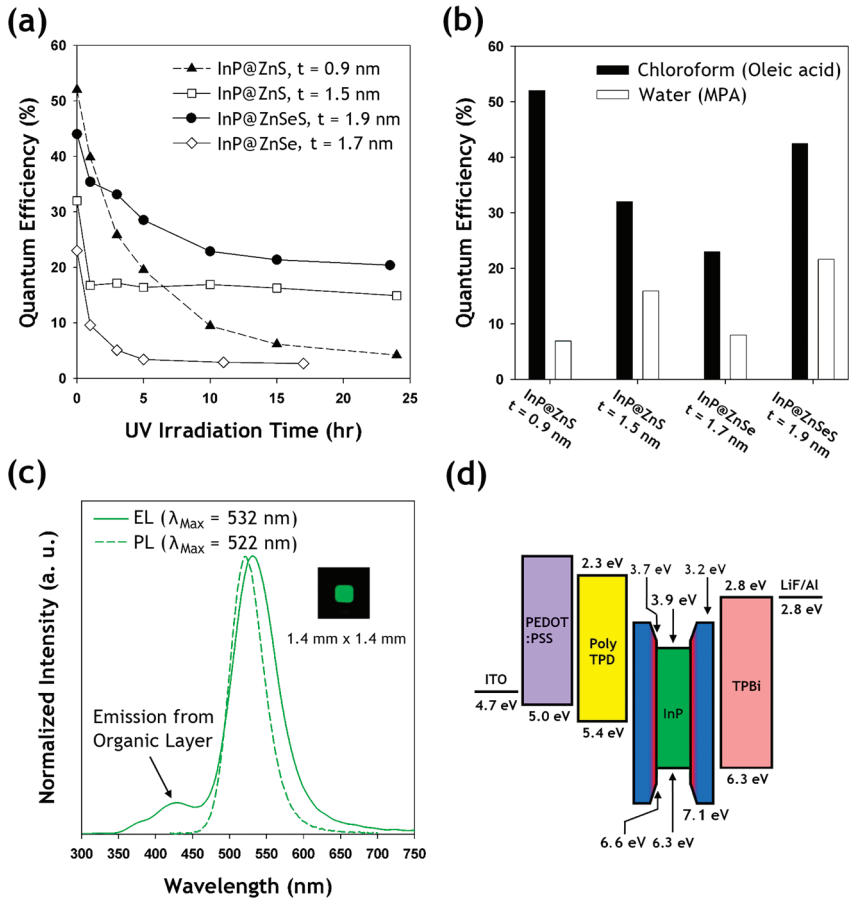

Figure 4. Effect of shell composition and thickness on QE against (a) UV irradiation in air (with 2 mW/cm^2 at 352 nm) and (b) ligand exchange with MPA. (c) PL spectrum of green light-emitting InP@ZnSeS QDs, an EL spectrum of QD-LEDs, and a photograph of a QD-LED (inset). (d) Energy-band diagram of the QD-LED presented in panel c. The theoretical values for the valence (or HOMO) and conduction bands (or LUMO) for individual layers were obtained from refs 1d and 8.

Moreover, the optimal molar ratio of TOPSe (r) remained in a narrow range and hardly changed ($0.05 \leq r \leq 0.2$), even if the amount of shell formation precursors (i.e., n) was increased. To clarify these unexpected results, we investigated the temporal evolution of QEs for three different shells (i.e., ZnS, ZnSeS, and ZnSe) made from $r = 0$, 0.05, and 1 with $n = 2$ fixed, as shown in Figure 2b. The gradual decrease after the maximum QE is observed in both cases of InP@ZnSe and InP@ZnS QDs, whereas InP@ZnSeS QDs, which are prepared with $r = 0.05$ and $n = 2$, do not exhibit any significant reduction in QE after the maximum value. The same tendency was also observed with smaller and larger n values, and the extent of QE reduction of both InP@ZnSe and InP@ZnS QDs becomes more pronounced as n increases (see Figures S2a and 2b in the Supporting Information). The gradual decrease in QE after 5−10 min of reaction is usually observed. Based on the high-resolution TEM images in Figure 3 and the core size estimated from the first exciton peak, ZnSeS alloy shells in the optimal condition turn out to consist of ~0.6 monolayers of ZnSe shell near the core and ~4.5 monolayers of ZnS outershell (see Table S3 in the Supporting Information). The thickest ZnSeS shell with an optimal molar ratio of TOPSe was estimated to be grown up to 1.9 nm in thickness (see Figure 3 and Table S3 in the Supporting Information). This estimated thickness is larger than the previously reported value (i.e., typical QDs with ZnS shells have shell thicknesses of <1 nm).[3e−g] Even with a rather thick shell, we minimized the lattice mismatch based on the composition gradient shells and, as a result, shells almost twice as thick were overgrown without causing the significant reduction in PL QE. The enhanced QE in the narrow range of the molar ratio of TOPSe (r) seems to originate from the uniformity of the shells. Ideally, the uniform shell growth can be achieved via thermodynamically controlled growth with materials lattice-matched to the core.[7] Although ZnSe is more relevant than ZnS, with respect to the lattice match, the faster growth of ZnSe shells than ZnS shells seems to be under kinetic control at a high concentration. Thermodynamically controlled growth is favored for the uniform shell growth. ZnS shell is favored thermodynamically but the uniform shell with it is difficult to achieve, because of a large lattice mismatch. We can guess that only a small fraction of TOPSe is needed to obtain the conformal growth of the ZnSeS composition gradient shells, with ZnSe acting as a lattice adaptor. In addition to the shell uniformity, it is also thought that insufficient conduction band offset between InP core and ZnSe shell (0.2−0.3 eV for green-emitting InP core and ZnSe[4a,8]) is responsible for the decreased QE in cases of large r, for the undesired delocalization of electron wave function to QD surface resulting nonradiative decay. This argument is supported by the fact that increasing r leads to a dramatic red-shift of PL spectra (see Figure S3 in the Supporting Information) and corresponding low QEs.

dx.doi.org/10.1021/cm201550w |*Chem. Mater.* 2011, 23, 4459–4463

The luminescent properties of QDs with a thick composition gradient shell are expected to be maintained under degradable conditions, such as surface oxidation by UV irradiation, rigorous purification, or surface modifications frequently done for practical usages. In order to investigate the enhancement in photo/chemical stability of QDs with the composition gradient shells, we treat them with rather harsh UV irradiation in the presence of oxygen, as shown in Figure 4a and carry the ligand exchange on InP@ZnSeS QDs (with a shell thickness of $t \approx 1.9$ nm), conventional InP@ZnS QDs ($t \approx 0.9$, 1.5 nm), and InP@ZnSe QDs ($t \approx 1.7$ nm) with 3-mercaptopropionic acid (MPA), respectively, shown in Figure 4b. We can notice that (i) InP@ZnSeS QDs exhibit the best QE under such illumination and surface modification stresses among other QDs and (ii) their QE reduction rate is significantly lower than that of other QDs. We think that the enhanced stability is due to the improved uniformity of composition gradient shells, the efficient confinement of exciton wave functions, and the minimized surface oxidation and nonradiative decay via surface states generated by photo-oxidation or ligand exchange. InP@ZnS QDs with thin shells and InP@ZnSe QDs with small conduction band offset show lower QE and stability, probably because of the thinner shell and the lower potential barrier, respectively. This is again ascertained by repeated shell growth experiments, as shown in Figure S4 in the Supporting Information. No considerable red shift is observed after the growth of ZnS shells over existing ZnSeS shells with $n = 4$, implying the efficient confinement of exciton wave functions. InP@ZnSeS QDs with the composition gradient shells also retained the same QE against rigorous purification steps (for eight precipitation and redispersion cycles), whereas InP@ZnS QDs with thin shells significantly changed from initially high QE (>50%) to 30% below, even after three purification step cycles. Using the InP@ZnSeS QDs with enhanced stability, we succeeded in fabricating InP-based colloidal green light-emitting devices (LEDs), as shown in Figures 4c and 4d (to the best of our knowledge, InP-based colloidal QLEDs have not been demonstrated so far). Its maximum external quantum efficiency (EQE) is ~0.008%, as shown in Figure S5 in the Supporting Information, and QDs have a full width at half maximum (fwhm) of 70 nm. There is still more room for improvement and optimization. The systematic study on the relationship between shell thickness and electronic properties of QD-LEDs is currently underway and will be discussed in more detail in a forthcoming paper.

In summary, by utilizing the reactivity difference between TOPSe and TOPS, we synthesized InP@ZnSeS QDs with a composition gradient in a radial direction. In terms of systematic investigation on the relationship between the shell nanostructure and QD stability, we demonstrated that QDs with thick gradient shells exhibited high QE and much-enhanced stability against the shell degradation under UV irradiation, ligand exchange, or rigorous purification. This enhanced stability of InP@ZnSeS QDs is attributed to the improved uniformity of composition gradient shells, the efficient confinement of exciton wave functions, and the minimized surface oxidation and nonradiative decay via surface states generated by photo-oxidation or ligand exchange. Using InP@ZnSeS QDs with enhanced stability, we were able to demonstrate InP-based colloidal green-emitting QD-LEDs. Although the current status of InP@ZnSeS QDs is not fully optimized to realize practical optoelectronic devices, the approach taken in the present study (i.e., the composition gradient shell structure naturally made from reactivity difference in precursors) will give clues to facilitate the synthesis of InP QDs with advanced nanostructures. Furthermore, the exploration of novel shell materials, such as Group III−V semiconductors (i.e., GaP, GaN), is underway to eliminate the heterogeneity between Group III−V cores and Group II−VI shells and, thus, improve the emission properties of InP-based QDs.

■ ASSOCIATED CONTENT

Supporting Information. Synthesis and device fabrication procedure, EDX analysis, high-resolution TEM images, estimation for shell thickness, $I-V$, $L-V$ characteristics, and EQE of QD-LEDs are provided as supplementary information. This material is available free of charge via the Internet at http://pubs.acs.org.

■ AUTHOR INFORMATION

Corresponding Author

*E-mail addresses: khchar@plaza.snu.ac.kr (K.C.), shnlee@snu.ac.kr (S.L.).

■ ACKNOWLEDGMENT

This work was financially supported by the National Research Foundation of Korea (NRF) funded by the Korea Ministry of Education, Science, and Technology (MEST) through BK21. SNU Brain Fusion and Korea Research Foundation (KRF) for artificial atoms research supported this work. The National Creative Research Initiative Center for Intelligent Hybrids (No. 2010-0018290) and the WCU (World Class University) Program of Chemical Convergence for Energy and Environment (R31-10013), the National Research Foundation of Korea Grant funded by the Korean Government (MEST) (No. NRF-2009-C1AAA001-2010-0028852), and the Technology Innovation Program funded by the Ministry of Knowledge Economy (MKE) (No. 20103020010020-11-2-200). This work was also in part supported by the International Research Training Group: Self Organized Materials for Optoelectronics, jointly supported by the DFG and NRF.

■ REFERENCES

(1) (a) Colvin, V. L.; Schlamp, M. C.; Alivisatos, A. P. *Nature* **1994**, *370*, 354–357. (b) Coe, S; Woo, W.-K.; Bawendi, M. G.; Bulovic, V. *Nature* **2002**, *420*, 800–803. (c) Sun, Q.; Wang, Y. A.; Li, L. S.; Wang, D.; Zhu, T.; Xu, J.; Yang, C.; Li, Y. *Nat. Photonics* **2007**, *1*, 717–722. (d) Bae, W. K.; Kwak, J.; Park, J. W.; Char, K.; Lee, C.; Lee, S. *Adv. Mater.* **2009**, *21*, 1690–1694. (e) Lee, J.; Sundar, V. C.; Heine, J. R.; Bawendi, M. G.; Jensen, K. F. *Adv. Mater.* **2000**, *12*, 1102–1105. (f) Jang, H. S.; Yang, H.; Kim, S. W.; Han, J. Y.; Lee, S.-G.; Jeon, D. Y. *Adv. Mater.* **2008**, *20*, 2696–2702.

(2) (a) Bruchez, M., Jr.; Moronne, M.; Gin, P.; Weiss, S.; Alivisatos, A. P. *Science* **1998**, *281*, 2013–2016. (b) Kim, S.; Lim, Y. T.; Soltesz, E. G.; De Grand, A. M.; Lee, J.; Nakayama, A.; Parker, J. A.; Mihaljevic, T.; Laurence, R. G.; Dor, D. M.; Cohn, L. H.; Bawendi, M. G.; Frangioni, J. V. *Nat. Biotechnol.* **2004**, *22*, 93–97, **2000**, *122*, 12142−12150. (c) Derfus, A. M.; Chan, W. C. W.; Bhatia, S. N. *Nano Lett.* **2004**, *4*, 11–18. (d) Medintz, I. L.; Uyeda, H. T.; Goldman, E. R.; Mattoussi, H. *Nat. Mater.* **2005**, *4*, 435.

(3) (a) Micic, O. I.; Curtis, C. J.; Jones, K. M.; Sprague, J. R.; Nozik, A. J. *J. Phys. Chem.* **1994**, *98*, 4966–4969. (b) Micic, O. I.; Smith, B. B.; Nozik, A. J. *J. Phys. Chem. B* **2000**, *104*, 12149–12156. (c) Haubold, S.; Haase, M.; Kornowski, A.; Weller, H. *ChemPhysChem* **2001**, *5*, 331–334. (d) Battaglia, D.; Peng., X. *Nano Lett.* **2002**, *2*, 1027–1030. (e) Xie, R.; Battaglia, D.; Peng, X. *J. Am. Chem. Soc.* **2007**, *129*, 15432–15433. (f) Li, L.; Reiss, P. *J. Am. Chem. Soc.* **2008**, *130*, 11588–11589. (g) Xu, S.; Ziegler, J.; Nann, T. *J. Mater. Chem.* **2008**, *18*, 2653–2656. (h) Xie, R.; Li,

Z.; Peng, X. *J. Am. Chem. Soc.* **2009**, *131*, 15457–15466. (i) Allen, P. M.; Walker, B. J.; Bawendi, M. G. *Angew. Chem., Int. Ed.* **2010**, *49*, 760–762. (j) Huang, K.; Demadrille, R.; Silly, M. G.; Sirotti, F.; Reiss, P.; Renault, O. *ACS Nano* **2010**, *4*, 4799–4805. (k) Borchert, H.; Haubold, S.; Haase, M.; Weller, H.; McGinley, C.; Riedler, M.; Moller, T. *Nano Lett.* **2002**, *2*, 151–154.

(4) (a) Cao, Y.; Banin, U. *J. Am. Chem. Soc.* **2000**, *122*, 9692–9702. (b) Kim, S.-W.; Zimmer, J. P.; Ohnishi, S.; Tracy, J. B.; Frangioni, J. V.; Bawendi, M. G. *J. Am. Chem. Soc.* **2005**, *127*, 10526–10532. (c) Aharoni, A.; Mokari, T.; Popov, I.; Banin, U. *J. Am. Chem. Soc.* **2006**, *128*, 257–264. (d) Choi, H. S.; Ipe, B. I.; Misra, P.; Lee, J. H.; Bawendi, M. G.; Frangioni, J. V. *Nano Lett.* **2009**, *9*, 2354–2359.

(5) (a) Holmes, J. D.; Ziegler, K. J.; Doty, R. C.; Pell, L. E.; Johnston, K. P.; Korgel, B. A. *J. Am. Chem. Soc.* **2001**, *123*, 3743–3748. (b) English, D. S.; Pell, L. E.; Yu, Z.; Barbara, P. F.; Korgel, B. A. *Nano Lett.* **2002**, *2*, 681–685. (c) Zou, J.; Baldwin, R. K.; Pettigrew, K. A.; Kauzlarich, S. M. *Nano Lett.* **2004**, *4*, 1181–1186. (d) Kang, Z.; Liu, Y.; Tsang, C. H. A.; Ma, D. D. D.; Fan, X.; Wong, N.-B.; Lee, S.-T. *Adv. Mater.* **2009**, *21*, 661–664.

(6) (a) Bae, W. K.; Char, K.; Hur, H.; Lee, S. *Chem. Mater.* **2008**, *20*, 531–539. (b) Bae, W. K.; Nam, M. K.; Char, K.; Lee, S. *Chem. Mater.* **2008**, *20*, 5307–5313. (c) Reiss, P.; Carayon, S.; Bleuse, J.; Pron, A. *Synth. Met.* **2003**, *139*, 649–652. (d) Talapin, D. V.; Mekis, I.; Gotzinger, S.; Kornowski, A.; Benson, O.; Weller, H. *J. Phys. Chem. B* **2004**, *108*, 18826–18831.

(7) McBride, S.; Treadway, J.; Feldman, L. C.; Pennycook, S. J.; Rosenthal, S. J. *Nano Lett.* **2006**, *6*, 1496–1501.

(8) Fu, H.; Zunger, A. *Phys. Rev. B* **1997**, *56*, 1496–1508.